Inorganic Chemistry

Article

pubs.acs.org/IC

Linker Conformation Effects on the Band Gap in Metal–Organic Frameworks

Espen Flage-Larsen*[,†,‡] and Knut Thorshaug[†]

[†]SINTEF Materials and Chemistry, P.O. Box 124 Blindern, Forskningsveien 1, N-0314 Oslo, Norway

[‡]Department of Physics, University of Oslo, 0313, Oslo, Norway

ABSTRACT: In this work, we investigate how torsion in the middle aromatic ring on the terphenyldicarboxylate linker in UiO-68 affects the band gap. Furthermore, we incorporate the effect of monosubstitution on the linker (UiO-68-R; R = H, F, I, NH_2, and NO_2) in order to shed light on a possible route to tune the band gap by changing the torsional angle by substitutions. Our computations show that both the torsional angle and band gaps depend on the choice of the substituent, and it is, in fact, possible to tune the band gap through the substitution's effect of locking down the middle aromatic ring at different torsional angles, in combination with the substituents' electronic effects.

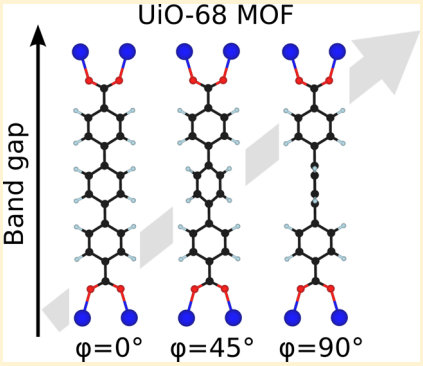

INTRODUCTION

Metal–organic frameworks (MOFs)[1] have received a considerable amount of attention in recent years. The wide range of applicable inorganic and organic building blocks has made it possible to prepare well-defined and highly porous yet stable materials with interesting properties in fields such as adsorption and separation,[2] sensing,[3] gas storage,[4] and catalysis.[5] However, their incorporation into electronic devices has been studied to a much lesser degree.[6]

It is well-known that the choice of the linker has an influence on the surface area and pore diameter of the MOF. For instance, in the series UiO-66, -67, and -68, the linker is dicarboxylate (UiO-66), biphenyldicarboxylate (UiO-67), and terphenyldicarboxylate (UiO-68). The resulting surface areas have been reported to be approximately 1400 m^2/g (UiO-66),[7] 2400 m^2/g (UiO-67),[7] and 4000 m^2/g (UiO-68).[8] Recently, we reported band gaps in the range 2.2–4.1 eV for MOFs described as UiO-6*x*-R MOFs (*x* = 6, 7, and 8; R = H, NH_2, and NO_2).[9] Our work shows that the linker also affects the band gaps.

The degree of conformational flexibility of the linker and its implications for the electronic properties are intriguing. From a fundamental point of view, it is of interest to understand how the microscopic structure and conformation relate to the macroscopic electronic properties of the MOF. From a more applied point of view and given the modular syntheses of MOFs, such an understanding may aid in the search for a bottom-up approach to design and prepare MOFs with predefined electronic properties. For example, band-gap tuning is of importance to the development of photocatalytically active MOFs.[10] Previous studies[11−13] show significant conformational effects on the electronic properties of biphenyl fragments and poly(*p*-phenylene), and this strongly motivated us to investigate these effects in MOFs.

Thus, herein we aim to contribute to the understanding of the relationship between the band gap and linker conformation in the MOF. By calculations, we investigate how the band gap is affected by rotation of the middle aromatic ring on the terphenyldicarboxylate linker in UiO-68, and we incorporate the effect of monosubstitution on the linker (UiO-68-R; R = H, F, I, NH_2, and NO_2).

The scheme used to investigate these effects is illustrated in Figure 1. First, we generated the UiO-68 structure based on our previous work,[9] illustrated in Figure 1a. Here, the middle aromatic ring is drawn in the planar configuration. The cell parameters of the relaxed cell were a = 23.333 Å, b = 23.319 Å, and c = 23.326 Å with angles α = 118.952°, β = 118.951°, and γ = 61.049°. This cell was used throughout this work. The middle aromatic ring was rotated according to Figure 1b, and the total energy and band gap were calculated using density functional theory (DFT).

COMPUTATIONAL DETAILS

Monosubstitution on the middle aromatic ring was studied for F, I, NO_2, and NH_2 (rotated 90° compared to the planar configuration as an input). The atomic coordinates were then fully relaxed in order to converge the F–C, I–C, and N–C (NH_2) and N–C (NO_2) distances (1.368, 2.118, 1.386, and 1.480 Å on average in this study) and bond angles. Then, in a second step, the middle aromatic ring was rotated without relaxing the atomic coordinates after rotation. The total energy and band gap were then extracted. In the third and final step, we relaxed all atomic coordinates for a selected set of input structures based on the most energetically stable configuration from step 2. In

Received: November 18, 2013
Published: February 14, 2014

   dx.doi.org/10.1021/ic4028628 | *Inorg. Chem.* 2014, 53, 2569–2572

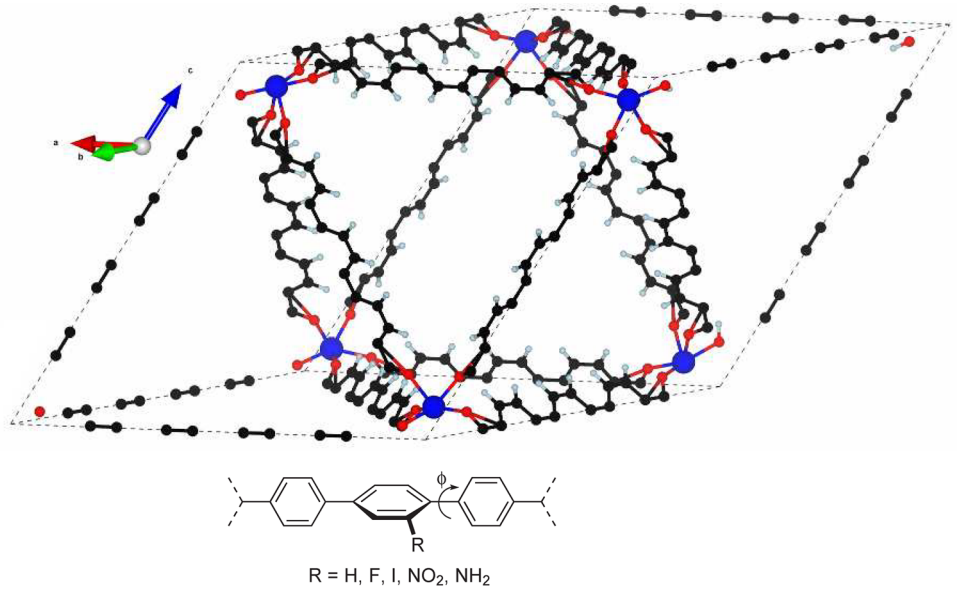

Figure 1. (top) Illustration of the triclinic unit cell of UiO-68 used throughout this work. Zirconium, oxygen, carbon, and hydrogen are shown in blue, red, black, and light-blue, respectively. (bottom) Rotation and substitution of the middle aromatic ring in the linker of the UiO-68 structure. For clarity, only the terphenyl fragment is shown.

addition, we performed relaxations of all atomic coordinates based on structures in step 2 that were not close to the most energetically stable configuration. These either relaxed to the same energetically stable minimum as the outcome of step 3 or did not converge within the time limits and force cutoff used in this work. The cell shape and volume were fixed during all calculations.

DFT calculations were performed using the Perdew–Burke–Ernzerhof[14] exchange-correlation functional in the Vienna ab Initio Simulation Package.[15,16] The conventional cubic unit cell for the UiO-68 structure[17] was converted to the primitive triclinic unit cell, containing 234 atoms for the hydroxylated configuration with hydrogen-terminated carbon linkers. For this primitive cell, an energy cutoff of 600 eV with a $\vec{k}$-point sampling of $3 \times 3 \times 3$ was used, and all relaxations were terminated when the residual forces were less than 5 meV/Å. Visualizations of the electron densities were generated in VESTA.[18] For all of the relaxed structures, there was a spread in the torsional angles (±2–10°). We thus only report the average value (dihedral angle measured on the substitutional side of the aromatic ring).

RESULTS AND DISCUSSION

The relative total energy and band gaps as a function of the torsional angle (ϕ) between the middle and outer aromatic rings are presented in parts a and b of Figure 2, respectively. The unsubstituted UiO-68-H shows significant energy dispersion across the torsional angles. The initial rotation yields a local minimum at 35°, while the fully relaxed energy minimum averaged at 34.1°, lowering the energy further by 0.24 eV. If we assume a similar energy dispersion between the unrelaxed and relaxed data sets, we see that the energy barrier for rotating ±15° out of the minimum is 0.20 eV and close to quadratic on both sides of the minimum. Furthermore, the energy barrier between the planar and most stable configuration is in excess of 0.6 eV. There are 6 linkers with 20 carbon atoms each in the unit cell, and thus the energy barrier of 0.2 eV is 0.03 eV per linker. We thus expect, even at room temperature (thermal energy of 0.04 eV/atom), spurious rotations of the middle aromatic rings. The aromatic ring contains 10 atoms. When the barrier exceeds approximately 0.40 eV, the aromatic linker in the UiO-68 structure should tend to stabilize in a more

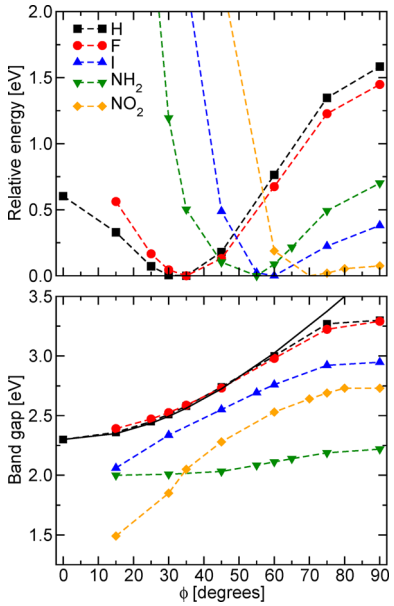

Figure 2. (upper) Relative total energy and (lower) band gap for rotations of the middle aromatic ring in the UiO-68-R structure (R = H, F, I, NH_2, and NO_2). The solid line in the lower panel is a cosine parametrization (see the text). Dashed lines are guides to the eye.

well-defined conformation (at room temperature). The conformation of the π orbitals in UiO-68-H favors the planar configuration. The reason for why the aromatic linker does not stabilize in this configuration is due to the repulsion between the electron density associated with the C–H bond on neighboring rings. For increasing torsional angles, the ideal π conformation (bonding and antibonding interactions) is partly destroyed until the system reaches the nonplanar configuration with the highest relative energy.

Moving on to the effects due to the substituents on the linker, i.e., the UiO-68-R, where R = F, I, NH_2, and NO_2, we see drastic differences in the energy dispersions compared to

dx.doi.org/10.1021/ic4028628 | Inorg. Chem. 2014, 53, 2569–2572

UiO-68-H. First, we notice that R = H and F yields similar energy dispersion curves, although the energy barrier is larger close to the planar configuration for R = F. Because of the increased electronegativity of F compared to H, the interaction close to the planar configuration is increased for F, which yields an increase in the energy barrier. The energy minimum for R = F is located at a similar, but slightly larger torsional angle compared to R = H. The fully relaxed minimum averaged at 39.3°, lowering the energy by 0.46 eV. Second, for R = I, NH_2, and NO_2, the aromatic ring does not want to reside in a planar configuration, or even close to it, as can be seen from the energy dispersion in Figure 2a. The total energy minimum for R = I, NH_2, and NO_2 is located at 60° (fully relaxed average of 53.7°, lowering the energy by 0.84 eV), 55° (fully relaxed average of 51.2°, lowering the energy by 0.83 eV), and 65° (fully relaxed average of 53.9°, lowering the energy by 1.27 eV), respectively. The dispersion around the energy minimum is significantly modified for R = I, NH_2, and NO_2 compared to R = H and F toward the planar configuration. This trend correlates nicely with the change in the electronegativity and interaction radius of the substitutes.

Compared to our previous study[9] of the band-gap modulations in the UiO-66 structure, we also here see a smaller band gap for the NH_2 analogue. Interestingly, the band gap changes drastically upon rotation of the aromatic ring, as can be seen in Figure 2; the band gap is smallest close to the planar configuration and largest close to its normal configuration. In its most stable conformation, UiO-68-H yields a band gap of 2.58 eV (2.60 eV for the fully relaxed minimum). For the planar configuration, parts of the carbon π states fully dominate the top valence band (except for the states located at −0.75 eV discussed in our previous work[9]). This is illustrated in Figure 3. Investigations of the bottom conduction band also reveal similar states. Upon rotation of the middle aromatic ring, the interaction between the carbon π states is modified. By inspection of the electron density associated with the carbon π states closes to the top valence band (see Figure 3), it is clear that the states associated with the least-bonding carbon π states are more delocalized in the planar compared to the nonplanar configuration. These states have been illustrated in previous work[19] (see Figure 3 in the reference) for poly(*p*-phenylenes), and they correlate nicely with our findings from the electron density in Figure 3.

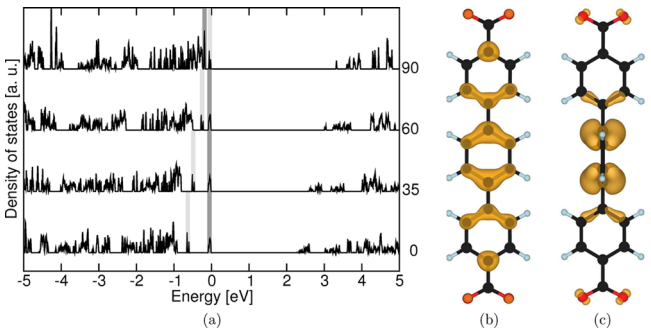

Figure 3. (a) Density of states for the UiO-68 structure with different torsional angles of the middle aromatic rings. (b) Electron density associated with the carbon π states in the top valence band (highlighted by dark gray in part a for the planar configuration). (c) Similar to part b but for the nonplanar configuration. Consult our previous work[9] for visualizations of the oxygen states highlighted by light gray. Oxygen, carbon, and hydrogen are shown in red, black, and light blue, respectively.

Furthermore, previous investigations[12,13,19] of phenyl chains concluded that the change in the band gap was due to a varying bandwidth stemming from the delocalized character of these states for both the valence and conduction bands. Except from the complications of additional states in our MOF structure and the fact that we have a supercell and folded bands (compared to previous work), it is reasonable to conclude a similar cause in these systems; in the planar configuration, the carbon π states are delocalized over the linker and interact with the lower-lying states. Upon rotation, the intraring interaction of the carbon π states is reduced, the bandwidth decreases, and the interaction with the lower-lying states is reduced. As a consequence, the band gap increases. This is also visible in Figure 3, where the states in the top valence and bottom conduction bands become more localized (sharper peaks in the density of states) in the nonplanar configuration where the band gap is the largest.

A cosine fit of the band gap as a function of the torsional angle is possible[19] using $E_g = E_0 + (E_{90} - E_0)[1 - \cos(\phi)]$, where E_0 and E_{90} are the magnitude of the band gap in the planar and nonplanar configurations, respectively. The origin of this cosine function can be developed from, for instance, Hückel theory. This fit is illustrated by the solid line in Figure 3 and shows behavior similar to that for the phenyl chains[13] at moderate torsional angles (below 60°). However, this fit is unsatisfactory as the torsional angle approaches 90°. This can be fully explained from the density of states in Figure 3, where the oxygen states define the top valence band for large torsional angles. These states are not present for phenyl chains, and it is thus reasonable that a simple cosine fit will fail in this range. In summary, for UiO-68, assuming that the nonplanar configuration cannot be reached, the band gap is determined by the least-bound carbon π states interacting with neighboring states between the aromatic rings.

An important question thus needs to be answered; is it possible to stabilize the aromatic ring in other rotational conformations and thus modify the band gap? We will in the following shed some light on this by investigating the results for the F, I, NO_2, and NH_2 substitutions. First, we note that dispersion of the energy and band gap is similar across all studied structures (i.e., increasing for increasing torsional angles). As for the rotational energy barrier, the variations in the band gap upon rotation are similar for R = H and F. However, for R = I, there is a significant shift in the band gap for all rotational angles. In its most stable state, UiO-68-I yields a band gap of 2.76 eV (2.68 eV for the fully relaxed structure). This is slightly higher than those for the most stable rotational angles for R = H and F and can be fully explained; I has a significantly larger interaction radius compared to H and F and will thus infer a stronger interaction between the C−I and nearby C−H electron density. Close to the planar configuration, the interaction with the nearby C−H electron density is particularly present (see the relative energy in Figure 2). The interaction is stronger than that for the F-substituted structure and forces the structure with R = I into an energy minimum with a larger band gap.

For the NO_2 substitutions, we note that, at first sight, compared to our previous study[9] for UiO-66, NO_2 substitutions in the UiO-68 structure yield a significantly smaller band gap compared to that of the unsubstituted structure. However, it is important to compare the band-gap values at the energy minima. In doing this, we find that NO_2 substitutions onto

dx.doi.org/10.1021/ic4028628 | Inorg. Chem. 2014, 53, 2569−2572

UiO-66[9] and UiO-68 have the same result, a rather small change in the band gap compared to the unsubstituted analogues. The NO_2 substituent itself relaxes (relaxations started from an aromatic rotation angle of 90°) not in a nonplanar configuration as in UiO-66[9] but with an average 42° tilt with respect to the plane of the middle aromatic ring. We investigated this energy minimum further by performing a calculation with the NO_2 tilted 90° compared to the planar middle aromatic ring. This resulted in an total energy increase of 0.38 eV with a band gap of 2.80 eV, which thus signifies a significant reduction of the stability of the structure. For NO_2, the most energetically stable configuration yields a band gap of 2.69 eV (2.54 eV for the fully relaxed structure).

Finally, for the R = NH_2 substitution, the band gap for the most stable configuration is 2.08 eV (2.04 eV for the fully relaxed structure). We put emphasis on the weaker band-gap dispersion present for NH_2 compared to the other substitutes; there is only a 0.2 eV difference in the band gap between the planar and nonplanar configurations. Because the difference between NH_2 and the other substitutes is an extra lone pair sitting close to the carbon, we believe this to be a significant factor for the reduced dispersion. These states dominate the top valence band, as seen in our previous study[9] (also confirmed in this study), and the $\pi-\pi$ intraring interactions are thus much less directly responsible for the band-gap changes.

In the end, it is worth pointing out the fact that the cosine fit would, for more complex substitutes, only be satisfactory in a very narrow range because of the strong interactions toward the planar configuration compared to the R = H structures. It can thus not be considered as a tractable approximation for more interacting and larger substitutes compared to hydrogen.

CONCLUSION

Rotation of the middle aromatic ring on the terphenyldicarboxylate linker in UiO-68-R (R = H, F, I, NH_2, and NO_2) significantly affects the band gap. Our calculations show strong band-gap modulations as a function of the torsional angle in the linker. We show that it is, in fact, possible to tune the band gap by placing various monosubstituents on the linker. This is due to the combination of the substitution's effect of locking down the middle aromatic ring at different torsional angles and the electronic influence exerted by the substituent.

AUTHOR INFORMATION

Corresponding Author

*E-mail: espen.flage-larsen@sintef.no.

Notes

The authors declare no competing financial interest.

ACKNOWLEDGMENTS

We gratefully acknowledge the NOTUR consortium for computational resources and SINTEF Materials and Chemistry for financial support.

REFERENCES

(1) Yaghi, O. M.; Li, H. L. *J. Am. Chem. Soc.* **1995**, *117*, 10401−10402.
(2) Li, J. R.; Kuppler, R. J.; Zhou, H. C. *Chem. Soc. Rev.* **2009**, *38*, 1477−1504.
(3) Kreno, L. E.; Leong, K.; Farha, O. K.; Allendorf, K.; van Duyne, R. P.; Hupp, J. T. *Chem. Rev.* **2012**, *112*, 1105−1125.
(4) Morris, R. E.; Wheatley, P. S. *Angew. Chem., Int. Ed.* **2008**, *47*, 4966−4981.
(5) Lee, J.; Farha, O. K.; Roberts, J.; Scheidt, K. A.; Nguyen, S. T.; Hupp, J. T. *Chem. Soc. Rev.* **2009**, *38*, 1450−1459.
(6) Allendorf, M. D.; Schwartzberg, A.; Stavila, V.; Talin, A. A. *Chem.—Eur. J.* **2011**, *17*, 11372−11388.
(7) Schaate, A.; Roy, P.; Godt, A.; Lippke, J.; Waltz, F.; Wiebcke, M.; Behrens, P. *Chem.—Eur. J.* **2011**, *17*, 6643−6651.
(8) Hafizovic, J.; Olsbye, U.; Lillerud, K. P.; Jacobsen, S.; Guillou, N. Metal Organic Framework Compounds. WO2009/133366A2, April 29, 2009.
(9) Flage-Larsen, E.; Røyset, A.; Cavka, J. H.; Thorshaug, K. *J. Phys. Chem. C* **2013**, *117*, 20610−20616.
(10) Gascon, J.; Hernandez-Alonso, M. D.; Almeida, A. R.; van Klink, G. P. M.; Kapteijn, F.; Mul, G. *ChemSusChem* **2008**, *1*, 981−983.
(11) Brock, C. P.; Minton, R. P. *J. Am. Chem. Soc.* **1989**, *111*, 4586−4593.
(12) Ambrosch-Draxl, C.; Majewski, J. A.; Vogl, P.; Leising, G. *Phys. Rev. B* **1995**, *51*, 9668−9676.
(13) Miao, M. S.; Camp, P. E. V.; Doren, V. E. V.; Ladik, J. J.; Mintmire, J. W. *J. Chem. Phys.* **1998**, *109*, 9623−9631.
(14) Perdew, J. P.; Burke, K.; Ernzerhof, M. *Phys. Rev. Lett.* **1996**, *77*, 3865−3868.
(15) Kresse, G.; Hafner, J. *Phys. Rev. B* **1993**, *47*, 558−561.
(16) Kresse, G.; Hafner, J. *Phys. Rev. B* **1994**, *49*, 14251−14269.
(17) Cavka, J. H.; Jakobsen, S.; Olsbye, U.; Guillou, N.; Lamberti, C.; Bordiga, S.; Lillerud, K. P. *J. Am. Chem. Soc.* **2008**, *130*, 13850−13851.
(18) Momma, K.; Izumi, F. *J. Appl. Crystallogr.* **2011**, *44*, 1272.
(19) Champagne, B.; Mosley, D. H.; Fripiat, J. G.; André, J.-M. *Phys. Rev. B* **1996**, *54*, 2381−2389.